

Stable High-Order Cubature Formulas for Experimental Data

Jan Glaubitz^a

^a*Department of Mathematics, Dartmouth College, Hanover, NH 03755, USA*

Abstract

In many applications, it is impractical—if not even impossible—to obtain data to fit a known cubature formula (CF). Instead, experimental data is often acquired at equidistant or even scattered locations. In this work, stable (in the sense of nonnegative only cubature weights) high-order CFs are developed for this purpose. These are based on the approach to allow the number of data points N to be larger than the number of basis functions K which are integrated exactly by the CF. This yields an $(N - K)$ -dimensional affine linear subspace from which cubature weights are selected that minimize certain norms corresponding to stability of the CF. In the process, two novel classes of stable high-order CFs are proposed and carefully investigated.

Keywords: Numerical integration, stable high-order cubature, experimental data, least squares, discrete orthogonal polynomials, ℓ^1 minimization

Contents

1	Introduction	1
2	What Do We Want? Stability and Exactness	3
3	Proposed Methods	6
4	Theoretical Results	9
5	Efficient Construction and Implementation	13
6	Numerical Results	14
7	Summary	19
	Appendix A	19
	Moments of the Monomials	

1. Introduction

Numerical integration is an omnipresent problem in mathematics and myriad other scientific areas. In fact, measuring areas and volumes dates back at least to the ancient Babylonians and Egyptians [2]. The present work is concerned with the determination—approximately or exactly—of integrals over regions in two or more dimensions. This problem was first studied in a systematic manner by Maxwell in 1877 [41] and is today known as *cubature*.

*Corresponding author: Jan Glaubitz

Email address: Jan.Glaubitz@Dartmouth.edu (Jan Glaubitz)

Let $\Omega \subset \mathbb{R}^q$ be a bounded domain with positive volume, $|\Omega| > 0$. Given N distinct data pairs $\{(\mathbf{x}_n, f_n)\}_{n=1}^N \subset \Omega \times \mathbb{R}$, we want to approximate the weighted integral

$$I[f] := \int_{\Omega} f(\mathbf{x})\omega(\mathbf{x}) \, d\mathbf{x} \quad (1)$$

with nonnegative weight function ω (assumed to be integrable) by an N -point CF

$$C_N[f] = \sum_{n=1}^N w_n f(\mathbf{x}_n). \quad (2)$$

Here, the distinct points $\{\mathbf{x}_n\}_{n=1}^N$ are called *data points* and the $\{w_n\}_{n=1}^N$ are called *cubature weights*. A sequence of CFs $(C_N)_{N \in \mathbb{N}}$ is called a *cubature rule (CR)*.

In one dimension ($q = 1$) the construction of CFs—usually referred to as *quadrature formulas (QFs)*—is dominated by the idea of interpolating the data (by a polynomial) and exactly integrating the polynomial then. Equidistant data points lead to Newton–Cotes, Chebyshev points to Clenshaw–Curtis and roots of Jacobi polynomials to Gauss–Jacobi rules [3, 7, 13, 22, 26, 38, 49]. These QFs can also be used to construct CFs for certain higher dimensional domains ($q > 1$) and weight functions, resulting in (generalized) Cartesian product rules [13].

Other approaches to construct CFs include minimal CFs, that are designed to be exact for (algebraic or trigonometric) polynomials of high degree using as few data points as possible; minimum-norm CFs, which are based on the idea to minimize the norm of the cubature error considered as a linear functional; and number-theoretical CFs, essentially derived from the ideas of Diophantine approximation and equidistribution modulo 1. We refer to a rich body of literature [9, 10, 13, 32, 37, 48] and references therein. Of course, this list is by no means exhaustive. Another important class of CFs are Monte Carlo (MC) and quasi Monte Carlo (QMC) methods [4, 15, 42]. In these, the data points are random samples (uniformly distributed over Ω) or correspond to partially or fully deterministic low-discrepancy sequences.¹ All of these methods have their own advantages and pitfalls. Yet, it should be stressed that most of the above formulas require a specific distribution of the data points.

In many applications, however, it is impractical—if not even impossible—to obtain data to fit a known CF [35, 45, 55]. For instance, experimental measurements are often performed at equidistant or even scattered locations. Furthermore, in some applications, numerical integration is a follow-up to some other task (e.g. numerically solving PDEs). In such a situation, it is not reasonable to require data points that are specific to a certain CF. The present work is therefore concerned with the construction of stable and high-order CF for general sets of data points.

1.1. State of the Art

At least in one dimension ($q = 1$), first steps towards such a goal have already been discussed in 1970 by Wilson. In [55], he proposed to construct stable high-order QFs by allowing the number of data points N to be larger than the desired degree of exactness (DoE) d . This yields an underdetermined least squares (LS) problem. While Wilson referred to the resulting QFs as *nearest point QFs*, in later works [26, 29, 36], the name *LS-QFs* was coined. Focusing on the constant weight function $\omega \equiv 1$ and equidistant data points, Wilson was able to show in [56] that stability of LS-QFs (in the sense of nonnegative only cubature weights) can be ensured essentially by choosing $N = (d + 1)^2$. In the process, Wilson utilized a beautiful connection between stable QFs and discrete orthogonal polynomials (DOPs). The connection between (Gaussian) QFs and continuous orthogonal polynomials (COPs), e.g., the Legendre polynomials, is well known. In contrast, the interplay between QFs and DOPs was—to the best of my knowledge—only developed further nearly 40 years later in [26, 27, 36]. In 2009, Huybrechs [36] revisited the original works of Wilson [55, 56] and conjectured that stability of these rules for $N \sim d^2$ should also hold for more general

¹These are supposed to enhance uniformity of the data points.

positive weight functions and scattered (not necessarily equidistant) data points. Recently, this was put on mathematically solid ground [26, Chapter 4] and an application of these QFs to numerical PDEs was explored in [29]. Furthermore, in [27], the idea of LS-QFs was utilized to construct stable QFs even for general weight functions (potentially having mixed signs).² Yet, to this date, no extension of these QFs to higher dimensions ($q > 1$) has been discussed.

1.2. Novel Contribution

The present work aims to construct stable high-order CFs for experimental data in two and more dimensions. These CFs assume a fixed set of data points as input and then aim to provide a stable numerical integration procedure. Moreover, the DoE of this numerical integration procedure is, in a certain sense, as high as possible. In particular, the proposed CFs satisfy a list of properties which are universally considered to be highly desirable [11, 12, 32, 38]:

- (P1) The data points lie in the integration domain Ω .
- (P2) The cubature weights are all nonnegative.
- (P3) The CF has a high (or even optimal) DoE for fixed data points.

Here, I propose two different methods to achieve this goal for fairly general bounded domains $\Omega \subset \mathbb{R}^q$. The first method transfers the idea of LS-QFs to higher dimensions. This approach is discussed in §3.2 and the resulting CFs will be called *LS-CFs*. They are essentially based on selecting a weighted LS solution from the solution space of the underdetermined linear system of exactness conditions (10). The second method, on the other hand, is based on selecting a least absolute values (ℓ^1) solution from the solution space. This method is presented in §3.1 and the resulting CFs will be referred to as ℓ^1 -CFs. These can provide higher DoE than LS-CFs (for the same set of data points). At the same time, however, they have to be determined iteratively and are therefore computationally more expensive.

Finally, it should be stressed that if the reader is only interested in evaluating some integral (1) and is *not* constrained to specific data points—the function values can be obtained at any desired location—there are certainly other CFs available for this purpose in most cases. The stable high-order CFs proposed in the present work, on the other hand, will find their greatest utility when it is difficult—or even impossible—to obtain data at locations required for a particular CF. The Matlab code corresponding to the methods developed in this work can be found at [25].

2. What Do We Want? Stability and Exactness

In many applications, it is not possible to get exact measurements $\{f_n\}_{n=1}^N$. Instead, we are left with *experimental measurements* $\{f_n^\varepsilon\}_{n=1}^N$ with *data error* (or *measurement error*)

$$\|\mathbf{f} - \mathbf{f}^\varepsilon\|_\infty \leq \varepsilon. \quad (3)$$

Here, \mathbf{f} and \mathbf{f}^ε respectively denote the vectors $(f_1, \dots, f_N)^T$ and $(f_1^\varepsilon, \dots, f_N^\varepsilon)^T$. In this case, we do not only have to ensure that the CF C_N is a good approximation of the exact integral I , but also that the growth of the data error is bounded and as small as possible. This can be observed from the following: If we estimate the error between the exact integral of f and the result of a CF applied to f^ε , we observe that

$$|I[f] - C_N[f^\varepsilon]| \leq |I[f] - C_N[f]| + |C_N[f] - C_N[f^\varepsilon]|. \quad (4)$$

²It should be pointed out that in this case stability holds in a weaker sense than compared to positive weight functions. In particular, it was argued in [27] that one should distinguish between stability and sign-consistency of QFs for general weight functions.

To the first term, we refer to as the *approximation error*. For the second term, we note that

$$|C_N[f] - C_N[f^\varepsilon]| \leq \varepsilon \sum_{n=1}^N |w_n|. \quad (5)$$

Thus, the second term is bounded by the data error ε times an amplification factor which depends on the cubature weights.³ This amplification factor is strongly connected to the stability of a CF and is minimal if the CF has nonnegative only cubature weights.

2.1. Stability

Given are two functions $f, f^\varepsilon : \Omega \rightarrow \mathbb{R}$ with $|f(\mathbf{x}) - f^\varepsilon(\mathbf{x})| \leq \varepsilon$ for all $\mathbf{x} \in \Omega$. Then, we have

$$|I[f] - I[f^\varepsilon]| \leq I[1]\varepsilon. \quad (6)$$

This means that the growth of errors in the input (data errors) are bounded by the factor $I[1]$.⁴ For an N -point CF, on the other hand, we have

$$|C_N[f] - C_N[f^\varepsilon]| \leq \kappa(\mathbf{w})\varepsilon, \quad \kappa(\mathbf{w}) = \sum_{n=1}^N |w_n|. \quad (7)$$

Here, the growth of data errors is bounded by the *stability value* $\kappa(\mathbf{w})$. The value $\kappa(\mathbf{w})$ is a usual stability measure for CRs and yields the following definition.

Definition 1 (Stable CRs). A CR $(C_N)_{N \in \mathbb{N}}$ with corresponding cubature weights $(\mathbf{w}_N)_{N \in \mathbb{N}}$ is said to be *stable* if $\kappa(\mathbf{w}_N)$ is uniformly bounded; that is,

$$\sup_{N \in \mathbb{N}} \kappa(\mathbf{w}_N) < \infty.$$

The above definition of stability carries some disadvantages. First, even though the error growth is bounded for increasing N , errors might still propagate by a large factor. Further, the above definition addresses a whole sequence of CFs for an increasing number of measurements. In many application, however, we are stuck with a fixed finite number of measurement (at scattered data points) and want to construct a single CF which works 'best' for this situation. Motivated by the error bound (6), the following stability concept (coined in [26, 27]) seems to be more appropriate.

Definition 2 (Perfectly Stable CFs). We call a CF C_N with cubature weights \mathbf{w} *perfectly stable* if $\kappa(\mathbf{w}) = I[1]$.

In fact, $\kappa(\mathbf{w}) = I[1]$ is the smallest possible stability value we can expect for a reasonable CF. To be more precise: Expecting the CF to treat constants exactly ($C_N[1] = I[1]$), we can note

$$\kappa(\mathbf{w}) \geq \sum_{n=1}^N w_n = I[1], \quad (8)$$

where equality takes place if and only if the cubature weights are nonnegative.

Definition 3 (Nonnegative CFs). A CF C_N with cubature weights $\{w_n\}_{n=1}^N$ is said to be *nonnegative* if

$$w_n \geq 0, \quad n = 1, \dots, N.$$

³Note that (5) relates to a special set of parameters in the Hölder inequality. Other choices are possible and discussed in Remark 12.

⁴Such errors may be round-off or truncation errors (if f is defined analytically), or errors of measurement or experiment when f is determined by a physical process.

Hence, we can note the following connection between perfectly stable and nonnegative CFs.

Lemma 4. *Let C_N be a CF that satisfies $C_N[1] = I[1]$. Then, the following are equivalent:*

- (a) C_N is perfectly stable
- (b) C_N is nonnegative

It should be stressed that the above equivalence between perfectly stable and nonnegative CFs is exclusive for nonnegative weight functions ω . For general weight functions, on the other hand, stable and sign-consistent⁵ rules should be considered as two separated classes. Finally, note that $C_N[1] = I[1]$ means that C_N has DoE 0.

2.2. Exactness

Another important design criterion for CFs, which is strongly connected to their accuracy, is exactness.

Definition 5 (The DoE). A CF C_N on $\Omega \subset \mathbb{R}^q$ is said to have (*polynomial*) *DoE* d if the *exactness condition*

$$C_N[f] = I[f] \quad \forall f \in \mathbb{P}_d(\mathbb{R}^q) \quad (9)$$

holds.⁶

Here, $\mathbb{P}_d(\mathbb{R}^q)$ denotes the vector space of all (algebraic) polynomials of degree at most d .

Remark 6. Note that an (algebraic) polynomial in q variables $\mathbf{x} = (x_1, \dots, x_q)$ is a finite linear combination of monomials of the form $\mathbf{x}^\alpha = x_1^{\alpha_1} \dots x_q^{\alpha_q}$ with the *degree* (also known as the *total degree*) defined as $|\alpha| = \sum_{i=1}^q \alpha_i$. Then, the (*total*) *degree of a polynomial* is the maximum of the degrees of its monomials. While we only focus on the total degree in this work, other choices would be possible as well. These include the *absolute degree* ($|\alpha|_\infty = \max_{i=1, \dots, q} \alpha_i$) and the *Euclidean degree* ($|\alpha|_2^2 = \sum_{i=1}^q \alpha_i^2$); see [50].

Exactness guarantees that polynomials up to a certain degree are treated exactly by the CF. Let $\{p_k\}_{k=1}^K$ be a basis of $\mathbb{P}_d(\mathbb{R}^q)$, where $K = \dim \mathbb{P}_d(\mathbb{R}^q) = \binom{d+q}{q}$. Then, the exactness condition (9) yields a system of linear equations (SLE)

$$\underbrace{\begin{pmatrix} p_1(\mathbf{x}_1) & \dots & p_1(\mathbf{x}_N) \\ \vdots & & \vdots \\ p_K(\mathbf{x}_1) & \dots & p_K(\mathbf{x}_N) \end{pmatrix}}_{=:P} \underbrace{\begin{pmatrix} w_1 \\ \vdots \\ w_N \end{pmatrix}}_{=:w} = \underbrace{\begin{pmatrix} m_1 \\ \vdots \\ m_K \end{pmatrix}}_{=:m}. \quad (10)$$

Here, $m_k := I[p_k]$ denotes the *m-th moment*. We can immediately note that a CF C_N has DoE d if and only if its weights solve (10). Let us assume $K < N$. Then, (10) becomes an underdetermined SLE. These are well-known to either have no solution or infinitely many. The existence of infinitely many solutions is ensured if the set of data points is $\mathbb{P}_d(\mathbb{R}^q)$ -unisolvent.

Definition 7 (Unisolvent Point Sets). A set of points $X = \{\mathbf{x}_n\}_{n=1}^N \subset \mathbb{R}^q$ is called $\mathbb{P}_d(\mathbb{R}^q)$ -*unisolvent* if

$$p(\mathbf{x}_n) = 0, \quad n = 1, \dots, N \implies p \equiv 0 \quad (11)$$

for all $p \in \mathbb{P}_d(\mathbb{R}^q)$. That is, the only polynomial of degree $\leq d$ that interpolates zero data is the zero polynomial.

⁵A CF is called *sign-consistent* if the signs of its weights match the signs of the weight function at the corresponding data points. That is, $\text{sign}(w_n) = \text{sign}(\omega(\mathbf{x}_n))$.

⁶Many authors add that the CF should be inexact for a polynomial of degree $d+1$. This results in uniqueness for the DoE: It is the largest number $d \in \mathbb{N}_0$ such that (9) holds. Following Definition 5, on the other hand, a CF which has DoE d also has DoE \tilde{d} for $\tilde{d} \leq d$. Yet, in the present discussion this will not yield any problems and we therefore proceed to use the slightly simpler Definition 5.

In this case, it is easy to note the following lemma.

Lemma 8. *Let $K = \dim \mathbb{P}_d(\mathbb{R}^q) < N$ and let $X = \{\mathbf{x}_n\}_{n=1}^N$ be $\mathbb{P}_d(\mathbb{R}^q)$ -unisolvent. Then, the SLE (10) is underdetermined and induces an $(N - K)$ -dimensional affine linear subspace of solutions*

$$W := \left\{ \mathbf{w} \in \mathbb{R}^N \mid P\mathbf{w} = \mathbf{m} \right\}. \quad (12)$$

Proof. Note that W can be rewritten as

$$W = \mathbf{w}_s + W_0, \quad W_0 := \left\{ \mathbf{w}_0 \in \mathbb{R}^N \mid P\mathbf{w}_0 = 0 \right\}.$$

Here, \mathbf{w}_s is a specific solution of $P\mathbf{w} = \mathbf{m}$ and W_0 is the linear solution space of the homogeneous problem. X being $\mathbb{P}_d(\mathbb{R}^q)$ -unisolvent results in the K columns of P being linearly independent. Thus, P has full rank and \mathbf{w}_s is ensured to exist. Finally, the rank-nullity theorem [46, Theorem 2.8] yields $\dim W_0 = N - K$ and therefore the assertion. \square

3. Proposed Methods

Given N data pairs $(\mathbf{x}_n, f_n^\varepsilon)_{n=1}^N \subset \Omega \times \mathbb{R}$, the aim is to construct perfectly stable (nonnegative) CFs with a high DoE. It should be stressed that this is done by first and foremost ensuring perfectly stability of the CF and optimizing the DoE only afterwards. This basic idea could be summarized as “*stability before exactness*”. In what follows, I present two methods to realize this strategy, resulting in—to the best of my knowledge—novel stable high-order CFs for scattered data points. Both procedures start with the following two steps:

- (S1) Determine the largest $d \in \mathbb{N}$ such that $X = \{\mathbf{x}_n\}_{n=1}^N$ is $\mathbb{P}_d(\mathbb{R}^q)$ -unisolvent.
- (S2) Formulate the SLE (10) for DoE d .

Note that for $K = \dim \mathbb{P}_d(\mathbb{R}^q) < N$ the SLE (10) becomes underdetermined. In this case, Lemma 8 ensures that (10) induces an $(N - K)$ -dimensional affine linear subspace of solutions W . Every element $\mathbf{w} \in W$ results in a CF with DoE d . The two methods below, resulting in ℓ^1 - and LS-CFs, aim to determine an element $\mathbf{w} \in W$ which also yields good stability properties.

3.1. ℓ^1 Cubature Formulas

Following the main goal—to ensure perfect stability—it seems natural to determine an element $\mathbf{w}^* \in W$ such that

$$\kappa(\mathbf{w}^*) \leq \kappa(\mathbf{w}) \quad \forall \mathbf{w} \in W. \quad (13)$$

Since $\kappa(\mathbf{w}) = \|\mathbf{w}\|_1$, the resulting optimization problem corresponds to ℓ^1 -minimization (which is strongly connected to compressed sensing [5, 6, 16, 28]). Thus, the element \mathbf{w}^* is called an ℓ^1 -*solution* from $W \subset \mathbb{R}^N$, which is denoted as

$$\mathbf{w}^{\ell^1} = \arg \min_{\mathbf{w} \in W} \|\mathbf{w}\|_1. \quad (14)$$

Once the cubature weights \mathbf{w}^{ℓ^1} have been computed, one checks whether the resulting CF is perfectly stable or not. This can be done either by directly examining perfect stability ($\kappa(\mathbf{w}^{\ell^1}) = I[1]$) or by inspect nonnegativity ($\mathbf{w}^{\ell^1} \geq 0$). If the resulting CF is perfectly stable, the desired integral $I[f]$ is approximated by the following ℓ^1 -CF:

$$C_N^{\ell^1}[f^\varepsilon] := \sum_{n=1}^N w_n^{\ell^1} f_n^\varepsilon \quad (15)$$

By construction, this CF is perfectly stable, while having DoE d . On the other hand, if the resulting CF is *not* perfectly stable, one decreases the DoE by one ($d \mapsto d - 1$) and returns to (S2). The whole procedure is summarized in Algorithm 1.

Algorithm 1 Construction of ℓ^1 -CFs

- 1: Determine the greatest $d \in \mathbb{N}$ such that X is $\mathbb{P}_d(\mathbb{R}^q)$ -unisolvent
 - 2: Formulate the SLE $P\mathbf{w} = \mathbf{m}$ for DoE d
 - 3: Compute an ℓ^1 -solution $\mathbf{w}^* = \arg \min_{\mathbf{w} \in W} \|\mathbf{w}\|_1$
 - 4: **while** $\mathbf{w}^{\ell^1} \not\geq 0$ **do**
 - 5: Reduce the DoE: $d = d - 1$
 - 6: Formulate SLE $P\mathbf{w} = \mathbf{m}$ for the decreased DoE d
 - 7: Compute an ℓ^1 -solution $\mathbf{w}^{\ell^1} = \arg \min_{\mathbf{w} \in W} \|\mathbf{w}\|_1$
 - 8: Approximate $I[f]$ by $C_N^{\ell^1}[f^\varepsilon]$ as in (15)
-

In my own implementation, I have utilized the stability criterion " $\mathbf{w}^{\ell^1} \geq 0$ ". This condition is expected to be more robust than " $\kappa(\mathbf{w}^{\ell^1}) = I[1]$ ", which can be sensitive to rounding errors if not implemented with care. While I think that Algorithm 1 better explains the basic idea, a computationally more efficient reformulation of the above procedure is described in Algorithm 3.

Remark 9 (Computation and Uniqueness of the ℓ^1 -Solution). It should be noted that $\|\cdot\|_1$ is a convex but not strictly convex norm. Hence, in general, the ℓ^1 -solution will not be unique. Yet, it is also well-known that in most cases this is not a problem and the ℓ^1 -solution, in fact, is unique. In many cases, the ℓ^1 -solution furthermore has the property of being a sparse solution; see [18, 19, 52] (also see [17]). In recent years, this motivated many researchers to use the ℓ^1 -norm as a surrogate for the " ℓ^0 -norm" (number of nonzero entries) [5, 6, 16, 28].⁷ In my own implementation, I used the Matlab function *minL1lin* [40] to solve (14). Please see [40] for more information.

3.2. Least Squares Cubature Formulas

Another option is to minimize a weighted ℓ^2 -norm instead of the ℓ^1 -norm. This approach is motivated by the wish to have—at least formally—an explicit representation for the cubature weights. The resulting vector of weights is referred to as the (*weighted*) *LS solution*:

$$\mathbf{w}^{\text{LS}} = \arg \min_{\mathbf{w} \in W} \left\| R^{-1/2} \mathbf{w} \right\|_2 \quad (16)$$

Here, the weight matrix $R^{-1/2}$ is given by

$$R^{-1/2} = \text{diag} \left(\frac{1}{\sqrt{r_1}}, \dots, \frac{1}{\sqrt{r_N}} \right), \quad r_n = \frac{\omega(\mathbf{x}_n)|\Omega|}{N} > 0, \quad (17)$$

and with $|\Omega|$ denoting the volume of $\Omega \subset \mathbb{R}^q$. This choice ensures the cubature weights to become nonnegative for an appropriate ratio between the DoE d and the number of data points N ; see Theorem 14. This is elaborated on in §4.

Regarding stability, the LS solution is expected to be inferior to the ℓ^1 solution, since $\kappa(\mathbf{w}^{\ell^1}) \leq \kappa(\mathbf{w}^{\text{LS}})$. Yet, the LS solution of an underdetermined SLE can be computed much more efficiently than an ℓ^1 solution. In particular, \mathbf{w}^{LS} is unique and has an explicit representation ([8]):

$$\mathbf{w}^{\text{LS}} = RP^T (PRP^T)^{-1} \mathbf{m} \quad (18)$$

Note that $RP^T (PRP^T)^{-1}$ is the Moore–Penrose pseudoinverse of $R^{-1/2}P$; see [1]. By utilizing a beautiful connection to DOPs, this formula can be considerably simplified; see §4.3.

⁷Of course, the " ℓ^0 -norm" is not really a norm—it is not absolutely homogenous—and the problem of computing ℓ^0 -solutions is NP-hard.

Note that once \mathbf{w}^{LS} has been computed, the procedure is the same as for the ℓ^1 -CFs: The DoE d is decreased until the LS solution (16) results in a perfectly stable CF. This CF is then referred to as the *LS-CF* and denoted by

$$C_N^{\text{LS}}[f^\varepsilon] := \sum_{n=1}^N w_n^{\text{LS}} f_n^\varepsilon. \quad (19)$$

The whole procedure is summarized in Algorithm 2.

Algorithm 2 Construction of LS-CFs

- 1: Determine the greatest $d \in \mathbb{N}$ such that X is $\mathbb{P}_d(\mathbb{R}^q)$ -unisolvent
 - 2: Formulate the SLE $P\mathbf{w} = \mathbf{m}$ for DoE d
 - 3: Compute the LS solution $\mathbf{w}^{\text{LS}} = \arg \min_{\mathbf{w} \in W} \left\| R^{-1/2} \mathbf{w} \right\|_2$
 - 4: **while** $\mathbf{w}^{\text{LS}} \not\geq 0$ **do**
 - 5: Reduce the DoE: $d = d - 1$
 - 6: Formulate the SLE $P\mathbf{w} = \mathbf{m}$ for the decreased DoE d
 - 7: Compute the LS solution $\mathbf{w}^{\text{LS}} = \arg \min_{\mathbf{w} \in W} \left\| R^{-1/2} \mathbf{w} \right\|_2$
 - 8: Approximate $I[f]$ by $C_N^{\text{LS}}[f^\varepsilon]$ as in (19)
-

Again, the loop of decreasing the DoE will be run through until a perfectly stable CF is found. In my own implementation, I computed the LS solution \mathbf{w}^{LS} using the Matlab function *lsqminnorm* instead of the explicit representation (30). Still, the matrix P is constructed from a basis of DOPs; see 4.2. In the later tests, this approach was found to be the numerically most stable one. Again, a computationally more efficient reformulation of the above procedure is described in Algorithm 3.

Remark 10. Perfect stability for the ℓ^1 and LS weights holds at latest for $d = 0$. In this case, there exists an ℓ^1 solution with a single nonzero weight $w_k^{\ell^1} = I[1]$ and $w_n^{\ell^1} = 0$ for $n \neq k$. The LS weights for $d = 0$, on the other hand, are uniquely given by $w_n^{\text{LS}} = \omega(\mathbf{x}_n) (\sum_{m=1}^N \omega(\mathbf{x}_m))^{-1} I[1]$; see §4 for more details.

3.3. Connection to Other Cubature Formulas

Let me point out certain connections of the above proposed ℓ^1 - and LS-CF to some well-known CFs.

Remark 11 (Minimum Norm CFs). The proposed approach might be best compared to *relative minimum-norm* CFs; see [47, Chapter 4 and 5] or the review [32] and references therein. Given a fixed set of data points X , these are constructed by considering the integration error $I[f] - C_N[f]$ as a linear functional and minimizing its operator norm. In comparison, in the present work, I aim to minimize the operator norm of the CF considered as a linear functional,

$$C_N : (\mathbb{R}^N, \|\cdot\|) \rightarrow (\mathbb{R}, |\cdot|), \quad \mathbf{f} \mapsto \mathbf{w} \cdot \mathbf{f} = \sum_{n=1}^N w_n f(\mathbf{x}_n). \quad (20)$$

If $\|\cdot\| = \|\cdot\|_\infty$, the operator norm of C_N is $\kappa(\mathbf{w})$, resulting in the ℓ^1 -CFs. For $\|\cdot\| = \|R^{-1/2} \cdot\|_2$, on the other hand, the operator norm of C_N is $\|R^{-1/2} \mathbf{w}\|_2$ and we get the LS-CFs.

Remark 12 (Alternative Stability Measures). Other choices for $\|\cdot\|$ are possible as well. Note that by Hölder's inequality,

$$|C_N[f]| \leq \|\mathbf{w}\|_p \|\mathbf{f}\|_q \quad (21)$$

for $1 < p, q < \infty$ with $1/p + 1/q = 1$. Equality holds if and only if the vectors $|\mathbf{w}|^p$ and $|\mathbf{f}|^q$ are linearly dependent. Here, $|\mathbf{v}|^p = (|v_1|^p, \dots, |v_N|^p)^T$ for $\mathbf{v} \in \mathbb{R}^N$. The operator norm of C_N is therefore given by $\|\mathbf{w}\|_p$. In this work, however, only the cases $p = 1$ and $p = 2$ are considered.

Remark 13 (Monte Carlo CFs). The LS-CF (19) can be seen as an high-order correction to (quasi) MC methods [4, 15, 42]. In these, the data points are obtained by (uniform) random samples and the weights are simply $w_n = |\Omega|\omega(\mathbf{x}_n)/N$. At the same time, it is shown in §4.3 that the LS weights are explicitly given by $w_n^{\text{LS}} = r_n \sum_{k=1}^K \pi_k(\mathbf{x}_n; \mathbf{r}) I[\pi_k(\cdot; \mathbf{r})]$, where $\{\pi_k(\cdot; \mathbf{r})\}_{k=1}^K$ is a basis of DOPs. For fixed K and an increasing number of data points, $\pi_k(\mathbf{x}_n; \mathbf{r}) I[\pi_k(\cdot; \mathbf{r})]$ converges to the Kronecker delta $\delta_{1,k}$. Hence, the difference between the MC and LS weights converges to zero then.

4. Theoretical Results

At least formally, the LS weights (16) are explicitly given by (18). It is not recommended to actually solve (18), however, since the normal matrix PRP^T is known to often be ill-conditioned. At the same time, (18) is also not handy for theoretical investigations. Yet, when we incorporate DOPs to formulate the SLE (10), it is possible to derive a simple explicit formula for the LS weights. Finally, this formula also yields the results that arbitrarily high DoEs are possible for the perfectly stable ℓ^1 - and LS-CFs.

4.1. Main Result and Consequences

The (theoretical) main result of this work is the following theorem, which states that for any fixed DoE d and a sufficiently large number N of $\mathbb{P}_d(\mathbb{R}^q)$ -unisolvent data points the LS weights (16) are all nonnegative.

Theorem 14. *Let $N_0 \in \mathbb{N}_0$ such that $X_{N_0} = \{\mathbf{x}_n\}_{n=1}^{N_0} \subset \Omega$ is $\mathbb{P}_d(\mathbb{R}^q)$ -unisolvent and $\omega(\mathbf{x}_n) > 0$ for $n = 1, \dots, N_0$. Moreover, for $N > N_0$, let $X_N = X_{N_0} \cup \{\mathbf{x}_n\}_{n=N_0+1}^N$ and $r_n = \omega(\mathbf{x}_n)|\Omega|/N$. Assume that*

$$\lim_{N \rightarrow \infty} \frac{|\Omega|}{N} \sum_{n=1}^N u(\mathbf{x}_n)v(\mathbf{x}_n)\omega(\mathbf{x}_n) = \int_{\Omega} u(\mathbf{x})v(\mathbf{x})\omega(\mathbf{x}) \, d\mathbf{x} \quad \forall u, v \in \mathbb{P}_d(\mathbb{R}^q). \quad (22)$$

Then, there exists an $N_1 \geq N_0$ such that for all $N \geq N_1$ the cubature weights (16) of the LS-CF with DoE d are all nonnegative.

The proof of the above theorem is provided in §4.4. The following corollary is a direct consequence of Theorem 14 and Lemma 4.

Corollary 15. *Let $d \in \mathbb{N}_0$. Under the same assumptions as in Theorem 14, there exists an $N_1 \in \mathbb{N}_0$ such that for all $N \geq N_1$ the following statements hold:*

- (a) *The LS-CF with cubature weights $\mathbf{w}^{\text{LS}} \in \mathbb{R}^N$ given by (16) is perfectly stable.*
- (b) *The ℓ^1 -CF with cubature weights $\mathbf{w}^{\ell^1} \in \mathbb{R}^N$ given by (14) is perfectly stable.*

The first statement follows from Lemma 4 and the second from the simple observation that $\kappa(\mathbf{w}^{\ell^1}) \leq \kappa(\mathbf{w}^{\text{LS}})$.

Remark 16. It should be stressed that (22) is a rather weak assumption on the (sequence) of data points. For instance, when the data points are obtained by (uniform) random samples, $\frac{|\Omega|}{N} \sum_{n=1}^N u(\mathbf{x}_n)v(\mathbf{x}_n)\omega(\mathbf{x}_n)$ corresponds to MC integration and (22) is ensured by the law of large numbers; see [13, Ch. 5.9]. Other options include low-discrepancy [4, 15, 42] and *equidistributed* (also called *uniformly distributed*) [39, 54] sequences of (partially or fully deterministic) data points.

4.2. Continuous and Discrete Orthogonal Polynomials

Let us consider the continuous inner product

$$\langle u, v \rangle = \int_{\Omega} u(\mathbf{x})v(\mathbf{x})\omega(\mathbf{x}) \, d\mathbf{x}, \quad (23)$$

which is induced by the nonnegative weight function ω . The corresponding norm is denoted by $\|\cdot\| = \sqrt{\langle \cdot, \cdot \rangle}$. If the inner product (23) is positive definite on $\mathbb{P}_d(\mathbb{R}^q)$ it induces a basis of orthogonal (OG) polynomials $\{\pi_k\}_{k=1}^K$, where $K = \dim \mathbb{P}_d(\mathbb{R}^q) = \binom{q+d}{d}$. That is, the polynomials $\{\pi_k\}_{k=1}^K$ satisfy

$$\langle \pi_k, \pi_l \rangle = \delta_{k,l}, \quad (24)$$

and span the space $\mathbb{P}_d(\mathbb{R}^q)$. These polynomials are referred to as *COPs* and denoted by $\pi_k(\cdot, \omega)$. Analogously, a discrete inner product is induced by

$$[u, v]_N = \sum_{n=1}^N r_n u(\mathbf{x}_n) v(\mathbf{x}_n), \quad (25)$$

where the $r_n \geq 0$ are nonnegative weights $r_n \geq 0$. This time, $\|[\cdot, \cdot]_N$ denotes the corresponding norm. Let us denote the set of all data points \mathbf{x}_n for which the corresponding weights r_n are positive by $X^+ = \{\mathbf{x}_n \in X \mid r_n > 0\}$. If this set is assumed to be $\mathbb{P}_d(\mathbb{R}^q)$ -unisolvent, the discrete inner product (25) is positive definite on $\mathbb{P}_d(\mathbb{R}^q)$ and induces a basis $\{\pi_k\}_{k=1}^K$ of so-called *DOPs*. These satisfy

$$[\pi_k, \pi_l]_N = \delta_{k,l}, \quad (26)$$

while spanning $\mathbb{P}_d(\mathbb{R}^q)$, and are denoted by $\pi_k(\cdot, \mathbf{r})$. Both OG bases can be constructed, for instance, by *Gram-Schmidt (GS) orthogonalization* [51]: Let $\{e_k\}_{k=1}^K$ be the set of monomials $e_k(\mathbf{x}) := \mathbf{x}^\alpha$ with $|\alpha| \leq d$. These are assumed to be ordered w. r. t. their degree. In particular, $e_1 \equiv 1$. Then, the OG polynomials are respectively constructed as

$$\begin{aligned} \tilde{\pi}_k(\mathbf{x}; \omega) &= e_k(\mathbf{x}) - \sum_{l=1}^{k-1} \langle e_k, \pi_l(\cdot; \omega) \rangle \pi_l(\mathbf{x}; \omega), & \pi_k(\mathbf{x}; \omega) &= \frac{\tilde{\pi}_k(\mathbf{x}; \omega)}{\|\tilde{\pi}_k(\cdot; \omega)\|}, \\ \tilde{\pi}_k(\mathbf{x}; \mathbf{r}) &= e_k(\mathbf{x}) - \sum_{l=1}^{k-1} [e_k, \pi_l(\cdot; \mathbf{r})]_N \pi_l(\mathbf{x}; \mathbf{r}), & \pi_k(\mathbf{x}; \mathbf{r}) &= \frac{\tilde{\pi}_k(\mathbf{x}; \mathbf{r})}{\|\tilde{\pi}_k(\cdot; \mathbf{r})\|_N}. \end{aligned} \quad (27)$$

Remark 17. Another option to construct bases of OG polynomials is the Stieltjes procedure [23]. For the numerical implementation, however, I recommend to use the *modified GS orthogonalization* [51] in which $\tilde{\pi}_k$ is computed by

$$\begin{aligned} \tilde{\pi}_k^{(1)} &= e_k - \langle e_k, \pi_1 \rangle \pi_1, \\ \tilde{\pi}_k^{(l)} &= \tilde{\pi}_k^{(l-1)} - \langle \tilde{\pi}_k^{(l-1)}, \pi_l \rangle \pi_l, \quad l = 2, \dots, k-1, \\ \tilde{\pi}_k &= \tilde{\pi}_k^{(k-1)} \end{aligned} \quad (28)$$

instead of $\tilde{\pi}_k = e_k - \sum_{l=1}^{k-1} \langle e_k, \pi_l \rangle \pi_l$, as displayed in (27).

For a more exhausting discussion of OG polynomials I highly recommend Gautschi's monograph [23].

4.3. Characterization of the Least Squares Solution

As noted before, at least formally, the LS solution (16) is given by (18). Yet, the real beauty of the LS approach is revealed when incorporating the concept of DOPs. In fact, the matrix product PRP^T in (18) can be identified as a Gram matrix w. r. t. the discrete inner product (25):

$$PRP^T = \begin{pmatrix} [p_1, p_1]_N & \cdots & [p_1, p_K]_N \\ \vdots & & \vdots \\ [p_K, p_1]_N & \cdots & [p_K, p_K]_N \end{pmatrix} \quad (29)$$

Let us formulate the matrix P and the vector of moments \mathbf{m} in the SLE (10) w.r.t. the basis of DOPs $\{\pi_k(\cdot, \mathbf{r})\}_{k=1}^K$. Then, $PRP^T = I$ and therefore

$$\mathbf{w}^{\text{LS}} = RP^T \mathbf{m}. \quad (30)$$

Thus, the LS weights \mathbf{w}^{LS} are explicitly given by

$$w_n^{\text{LS}} = r_n \sum_{k=1}^K \pi_k(\mathbf{x}_n; \mathbf{r}) I[\pi_k(\cdot; \mathbf{r})], \quad n = 1, \dots, N. \quad (31)$$

In particular, this formula makes it possible to subsequently prove that the LS weights are all nonnegative for fixed d and a sufficiently large set of data points.

4.4. Proof of the Main Results

Let me start with two preliminary results on the convergence of discrete inner products and the induced DOPs.

Lemma 18. *Assume that*

$$\lim_{N \rightarrow \infty} [u, v]_N = \langle u, v \rangle \quad \forall u, v \in \mathbb{P}_d(\mathbb{R}^q). \quad (32)$$

Moreover, let $(u_N)_{N \in \mathbb{N}}$ and $(v_N)_{N \in \mathbb{N}}$ be two sequences in $\mathbb{P}_d(\mathbb{R}^q)$ with

$$u_N \rightarrow u, \quad v_N \rightarrow v \text{ in } L^\infty(\Omega) \quad (33)$$

for $N \rightarrow \infty$, where $u, v \in \mathbb{P}_d(\mathbb{R}^q)$ and $\Omega \subset \mathbb{R}^q$. Then,

$$\lim_{N \rightarrow \infty} [u_N, v_N]_N = \langle u, v \rangle. \quad (34)$$

Proof. Note that

$$|\langle u, v \rangle - [u_N, v_N]_N| \leq |\langle u, v \rangle - [u, v]_N| + |[u, v]_N - [u_N, v]_N| + |[u_N, v]_N - [u_N, v_N]_N|. \quad (35)$$

The first term on the right hand side converges to zero due to (32). For the second term, the Cauch–Schwarz inequality gives

$$|[u, v]_N - [u_N, v]_N|^2 = |[u - u_N, v]_N|^2 \leq \|u - u_N\|_N^2 \|v\|_N^2.$$

Furthermore, (32) implies $\|v\|_N^2 \rightarrow \|v\|^2$ for $N \rightarrow \infty$. Finally, the Hölder inequality and (33) yield

$$\|u - u_N\|_N^2 \leq \|1\|_N^2 \|u - u_N\|_{L^\infty(\Omega)}^2 \rightarrow 0, \quad N \rightarrow \infty.$$

Thus, the second term converges to zero as well. A similar argument can be used to show that the third term converges to zero. \square

Next, it is shown that, when the discrete inner product (25) converges to the continuous inner product (23) for all polynomials of degree at most d , the DOPs $\pi_k(\cdot, \mathbf{r})$ converge uniformly to the COPs $\pi_k(\cdot, \omega)$.

Lemma 19. *Assume that*

$$\lim_{N \rightarrow \infty} [u, v]_N = \langle u, v \rangle \quad \forall u, v \in \mathbb{P}_d(\mathbb{R}^q). \quad (36)$$

For $k = 1, \dots, K$, let $\pi_k(\cdot; \mathbf{r})$ and $\pi_k(\cdot; \omega)$ respectively denote the k -th DOP and COP constructed by GS orthogonalization (27). Then, we have

$$\pi_k(\cdot; \mathbf{r}) \rightarrow \pi_k(\cdot; \omega) \text{ in } L^\infty(\Omega) \quad (37)$$

for $N \rightarrow \infty$ and $k = 1, \dots, K$.

Proof. The assertion is proven by induction. For $k = 1$ the assertion is trivial and essentially follows from $\|1\|_N \rightarrow \|1\|$, $N \rightarrow \infty$. Next, assuming that the assertion holds for the first $k - 1$ OG polynomials, it is argued that it also holds for the k -th OG polynomial. Assume

$$\pi_l(\cdot; \mathbf{r}) \rightarrow \pi_l(\cdot; \omega) \text{ in } L^\infty(\Omega), \quad N \rightarrow \infty, \quad (38)$$

holds for $l = 1, \dots, k - 1$. By the GS orthogonalization, the k -th OG polynomials are given by (27). Lemma 18 implies

$$[e_k, \pi_l(\cdot; \mathbf{r})]_N \rightarrow \langle e_k, \pi_l(\cdot; \omega) \rangle, \quad l = 1, \dots, k - 1, \quad (39)$$

and therefore

$$\tilde{\pi}_k(\cdot; \mathbf{r}) \rightarrow \tilde{\pi}_k(\cdot; \omega) \text{ in } L^\infty(\Omega), \quad N \rightarrow \infty. \quad (40)$$

Furthermore, Lemma 18 yields $\|\tilde{\pi}_k(\cdot; \mathbf{r})\|_N \rightarrow \|\tilde{\pi}_k(\cdot; \omega)\|$ for $N \rightarrow \infty$. This implies

$$\pi_k(\cdot; \mathbf{r}) \rightarrow \pi_k(\cdot; \omega) \text{ in } L^\infty(\Omega), \quad N \rightarrow \infty, \quad (41)$$

which completes the proof. \square

The previous two lemmas are next utilized to prove the main result (Theorem 14).

Proof of Theorem 14. Recall that the LS weights \mathbf{w}^{LS} are explicitly given by (31). Defining

$$\varepsilon_k := [\pi_k(\cdot; \mathbf{r}), 1]_N - \langle \pi_k(\cdot; \mathbf{r}), 1 \rangle, \quad (42)$$

the LS weights can be rewritten as

$$w_n^{\text{LS}} = r_n \left(\pi_1(\mathbf{x}_n; \mathbf{r}) [\pi_1(\cdot; \mathbf{r}), 1]_N - \sum_{k=1}^K \varepsilon_k \pi_k(\mathbf{x}_n; \mathbf{r}) \right). \quad (43)$$

Assuming the DOPs $\{\pi_k(\cdot; \mathbf{r})\}_{k=1}^K$ are ordered, one has $\pi_1(\cdot; \mathbf{r}) \equiv 1/\|1\|_N$. This yields

$$\pi_1(\mathbf{x}_n; \mathbf{r}) [\pi_1(\cdot; \mathbf{r}), 1]_N = [\pi_1(\cdot; \mathbf{r}), \pi_1(\cdot; \mathbf{r})]_N = 1. \quad (44)$$

Since $r_n > 0$, the assertion $w_n^{\text{LS}} \geq 0$ is therefore equivalent to

$$\sum_{k=1}^K \varepsilon_k \pi_k(\mathbf{x}_n; \mathbf{r}) \leq 1. \quad (45)$$

By (22) the discrete inner product $[\cdot, \cdot]_N$ converges to the continuous inner product $\langle \cdot, \cdot \rangle$ for all polynomials of degree at most d and Lemma 19 implies that

$$\pi_k(\cdot; \mathbf{r}) \rightarrow \pi_k(\cdot; \omega) \text{ in } L^\infty(\Omega) \quad (46)$$

for $N \rightarrow \infty$ and $k = 1, \dots, K$. In particular, the DOPs are uniformly bounded and there exists a constant $C > 0$ such that $|\pi_k(\mathbf{x}; \mathbf{r})| \leq C$ for all $\mathbf{x} \in \Omega$ and $k = 1, \dots, K$. Thus,

$$\sum_{k=1}^K \varepsilon_k \pi_k(\mathbf{x}_n; \mathbf{r}) \leq C \sum_{k=1}^K |\varepsilon_k|. \quad (47)$$

Since uniform convergence (46) holds, Lemma 18 yields $\varepsilon_k \rightarrow 0$, $N \rightarrow \infty$, for $k = 1, \dots, K$. Hence, there exists an $N_1 \geq N_0$ such that

$$|\varepsilon_k| \leq \frac{1}{CK}, \quad k = 1, \dots, K, \quad (48)$$

for $N \geq N_1$. Finally, this implies

$$\sum_{k=1}^K \varepsilon_k \pi_k(\mathbf{x}_n; \mathbf{r}) \leq 1 \quad (49)$$

and therefore the assertion. \square

5. Efficient Construction and Implementation

Below, some comments on computational aspects of the proposed LS- and ℓ^1 -CFs are provided. The corresponding Matlab code, which was also used to produce the subsequent numerical tests, can be found at [25].

5.1. Computation of the Moments

In my own implementation, I computed the matrix P from a basis of DOPs corresponding to (25). The DOPs are constructed by the modified GS procedure applied to the initial basis of monomials (see Remark 17). The corresponding moments can be computed, for instance, by using some available CF on Ω . Such an approach has been discussed, for instance, in [21] (also see [27] for general weight functions). Note that for the evaluation of the DOPs, one is not limited to the set of data points. Another approach, which I utilized in my implementation, is to compute the DOP's moments together with the DOPs from the modified GS procedure. Assuming that the moments of the monomials (or some other initial basis) are known, the GS iteration for the moments reads

$$I[\tilde{\pi}_k(\cdot; \mathbf{r})] = I[e_k] - \sum_{l=1}^{k-1} [e_k, \pi_l(\cdot; \mathbf{r})]_N I[\pi_l(\cdot; \mathbf{r})], \quad I[\pi_k(\cdot; \mathbf{r})] = \frac{I[\tilde{\pi}_k(\cdot; \mathbf{r})]}{\|\tilde{\pi}_k(\cdot; \mathbf{r})\|_N} \quad (50)$$

for $k = 1, \dots, K$. Again, I recommend the modified version (28) of the GS procedure. Finally, note that for many domains and weight functions, the monomial's moments can be found in the literature; see [9, 13, 20, 32] and references therein.

5.2. Finding Stable Cubature Formulas

Algorithms 1 and 2 describe a simple procedure to respectively determine the stable ℓ^1 - and LS-CF. The idea behind these is to start with the highest possible d such that the set of data points is still $\mathbb{P}_d(\mathbb{R}^q)$ -unisolvent. Then, the DoE d is decreased until the resulting CF is also ensured to be perfectly stable. In the later numerical tests, however, I found the final DoE of these CFs to usually be significantly smaller than the highest possible d such that the set of data points is $\mathbb{P}_d(\mathbb{R}^q)$ -unisolvent. This is in accordance with prior works in one dimension [26, 29, 36, 56]. Hence, in my own implementation, instead of Algorithms 1 and 2, I utilized the following algorithm to construct ℓ^1 - and LS-CFs.

Algorithm 3 Efficient Construction of ℓ^1 - and LS-CFs

- 1: $d, r, K, w_{\min} = 0$
 - 2: **while** $r = K$ and $w_{\min} \geq 0$ **do**
 - 3: Increase the DoE: $d = d + 1$
 - 4: $K = \binom{d+q}{q}$
 - 5: Formulate the SLE $P\mathbf{w} = \mathbf{m}$ for DoE d
 - 6: Compute the rank of P : $r = \text{rank}(P)$
 - 7: Compute the ℓ^1 /LS-solution \mathbf{w}^*
 - 8: Determine the smallest weight: $w_{\min} = \min(\mathbf{w}^*)$
 - 9: Decrease the DoE: $d = d - 1$
 - 10: Formulate the SLE $P\mathbf{w} = \mathbf{m}$ for DoE d
 - 11: Compute the ℓ^1 /LS-solution \mathbf{w}^*
 - 12: Approximate $I[f]$ by the corresponding ℓ^1 /LS-CF
-

Note that $\text{rank}(P) = K$ with $K = \binom{d+q}{q}$ is equivalent to X being $\mathbb{P}_d(\mathbb{R}^q)$ -unisolvent. Moreover, in my own implementation, I first computed the LS-CF and only afterwards the ℓ^1 -CF. Recall that the ℓ^1 -CF is ensured to at least have the same—yet, usually a higher—DoE than the LS-CF. Denoting the DoE of the LS-CF by d_{LS} , it therefore seems reasonable (more efficient) to initialize Algorithm 3 with $d = d_{\text{LS}}$ instead of $d = 0$ for computing the corresponding ℓ^1 -CF.

5.3. Computational Costs

The following list addresses the computational complexity of determining the LS cubature weights w. r. t. the number of data points N , the DoE d , and the dimension q .

- *Computation of the DOPs:* To formulate the matrix P , we need the values of the $K = \binom{d+q}{d}$ DOPs spanning $\mathbb{P}_d(\mathbb{R}^q)$ at the N data points $\{\mathbf{x}_n\}_{n=1}^N$. This is done by the modified GS process, which yields asymptotic costs of $\mathcal{O}(NK^2)$; see [31, Chapter 5.2.8].
- *Computation of the moments:* The moments $\{m_k\}_{k=1}^K$ are computed together with the DOPs by the modified GS process. Hence, the asymptotic costs are $\mathcal{O}(NK^2)$ as well.
- *Computation of the LS weights:* The LS weights $\{w_n^{\text{LS}}\}_{n=1}^N$ can be computed as in (30) by a simple matrix vector multiplication. Since R is a diagonal matrix, this is done with asymptotic costs of $\mathcal{O}(NK)$.

Altogether, the computational complexity of determining the LS weights is given by

$$\underbrace{\mathcal{O}(NK^2)}_{\text{DOPs}} + \underbrace{\mathcal{O}(NK^2)}_{\text{moments}} + \underbrace{\mathcal{O}(NK)}_{\text{LS weights}} = \mathcal{O}(NK^2). \quad (51)$$

Hence, the computational complexity is linear in N and quadratic in K . Moreover, it is worth noting that $\mathcal{O}(K) = \mathcal{O}(d^q)$. Finally, in the subsequent numerical tests, the ratio between d and N is investigated (see §6.1). Unfortunately, at least to me, the computational costs for computing the LS or ℓ^1 weights are less clear when optimization tools—in our case the Matlab functions *lsqminnorm* and *minL1lin*—are used.⁸

6. Numerical Results

In this section, the proposed stable high-order CFs are numerically investigated for a variety of different test cases. Among these are the (hyper-)cube $C_q = [-1, 1]^q$ and ball $B_q = \{\mathbf{x} \in \mathbb{R}^q \mid \|\mathbf{x}\|_2 \leq 1\}$ in two and three dimensions ($q = 2, 3$). The volumes of these domains are respectively given by $|C_q| = 2^q$ and $|B_q| = (\pi^{\frac{q}{2}})/\Gamma(\frac{q}{2} + 1)$. Here, Γ denotes the usual gamma function (see [24, Chapter 5.1], [30, Chapter 12.2], or [44, Chapter 5]). Moreover, each of these domains is equipped with two different weight functions. The cube is considered together with the weight functions $\omega \equiv 1$ and $\omega(\mathbf{x}) = \prod_{i=1}^q \sqrt{1 - x_i^2}$ (corresponding to products of *Chebyshev functions of second kind* [44, Chapter 18]; apart from a multiplicative constant, also known as the *Wigner semicircle distribution*). For the ball, the weight functions $\omega \equiv 1$ and $\omega(\mathbf{x}) = \sqrt{\|\mathbf{x}\|_2}$ are considered. The corresponding moments of the monomials can be found in Appendix A.

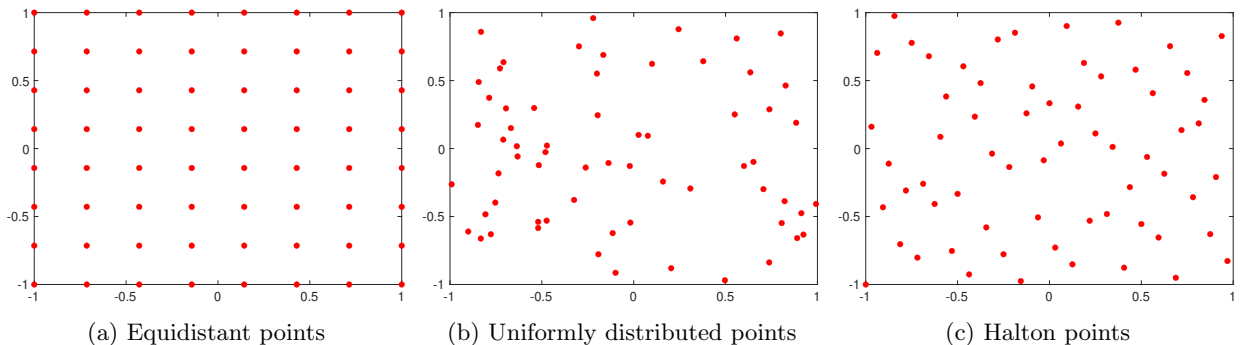


Figure 1: Illustration of three different types of $N = 64$ data points for the two-dimensional cube $C_2 = [-1, 1]^2$

⁸Any hint concerning this matter would be highly welcome.

Furthermore, three different types of data points are considered: (1) equidistant points, which are fully deterministic; (2) uniformly distributed points, which are fully random; and (3) Halton points [33], which are quasi-random and belong to the family of so-called *low discrepancy sequences*.⁹ Such points are developed to minimize the upper bound provided by the Koksma–Hlawak theorem [34, 43] and yield the rate of convergence of the MC method to increase from $1/2$ to essentially 1 ; see [4, 15, 50] and references therein. An illustration of these points in two dimensions is provided by Figure 1. For the corresponding (hyper-)ball, the subset of points with radius not greater than 1 is selected.

6.1. The Ratio Between N and d

First, the ration between the number of data points N and the DoE d is investiaged. Remember that d and the number of basis functions spanning $\mathbb{P}_d(\mathbb{R}^q)$ is related by $K = \binom{d+q}{q}$. Hence, the asymptotic relation $K \sim d^q$ holds. That is, $\lim_{d \rightarrow \infty} K/d^q = 1$ ([14, Chapter 1.4]). Table 1 reports on the relation between N and d for the LS- and ℓ^1 -CF on the two- and three-dimensional cube and ball. This relation is assumed to be of the form $N \approx Cd^s$. Here, the values for s and C have been determined numerically by performing an LS fit for $N = n^2$ with $n = 4, 8, \dots, 40$ in two dimensions and for $N = n^3$ with $n = 4, 5, \dots, 20$ in three dimensions.

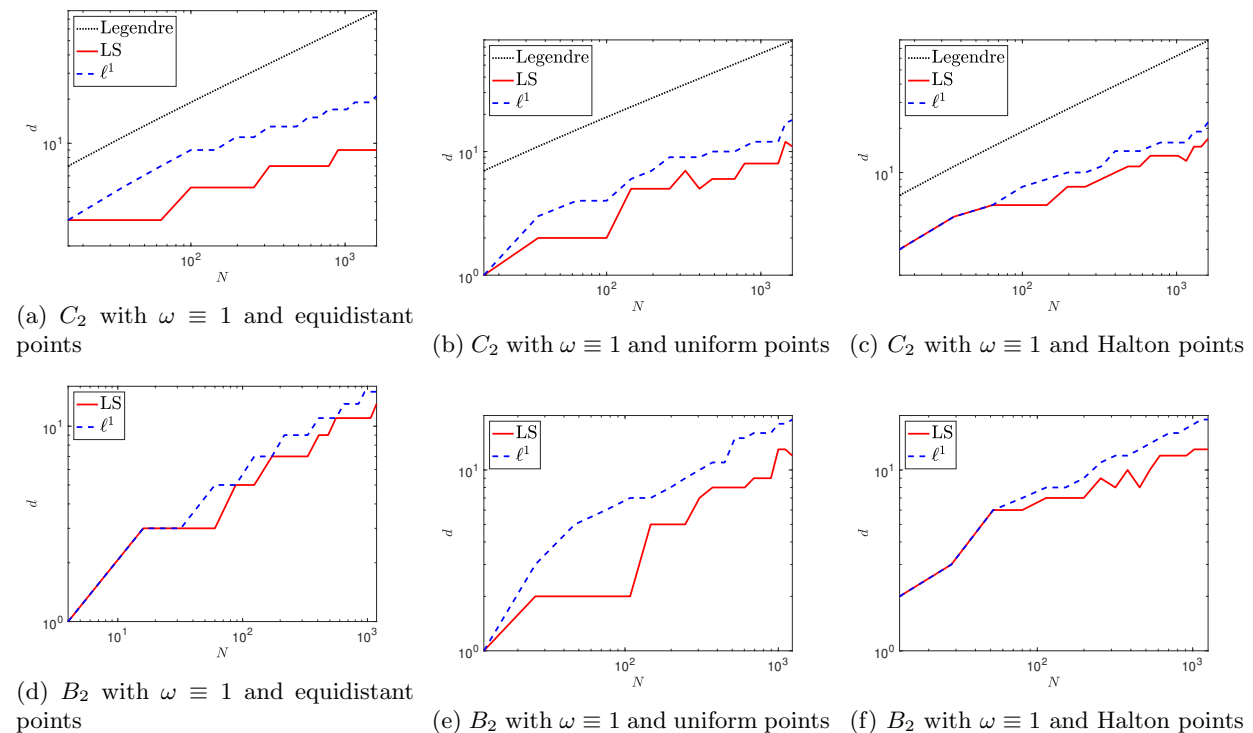


Figure 2: N versus d for C_2 and B_2 with $\omega \equiv 1$

Furthermore, for the cube and the weight function $\omega \equiv 1$, the asymptotic ratio of the LS- and ℓ^1 -CF is compared with the one of the product Legendre rule. This rule is known to provide DoE $d = 2n - 1$ if n Legendre points are used in every direction ($N = n^q$). Hence, $N \sim 2^{-q}d^q$ holds for the product Legendre rule. Unfortunately, some of the results are hard to compare. Yet, it can, for instance, be noted that going over from $\omega \equiv 1$ to one of the other two weight functions does not significantly change the ration between N and d . The same holds when comparing the results for the cube with the results for the ball. Even when the

⁹The Halton points generalize the one-dimensional van der Corput points; see [53, Erste Mitteilung] or [39].

LS-CF on the Cube

q		$\omega \equiv 1$			$\omega(\mathbf{x}) = (1 - x_1^2)^{1/2} \dots (1 - x_q^2)^{1/2}$			
		Legendre	equid.	uniform	Halton	equid.	uniform	Halton
2	s	2.0	3.3	1.6	2.4	3.0	1.9	2.4
	C	0.3	8.0e-1	2.6e+1	1.6	7.9e-1	2.3e+1	1.0
3	s	3.0	1.6	3.3	4.0	3.2	2.5	3.7
	C	1.2e-1	4.2e+2	5.5	2.0e-1	8.0	5.5e+1	6.5e-1

 ℓ^1 -CF on the Cube

q		$\omega \equiv 1$			$\omega(\mathbf{x}) = (1 - x_1^2)^{1/2} \dots (1 - x_q^2)^{1/2}$			
		Legendre	equid.	uniform	Halton	equid.	uniform	Halton
2	s	2.0	2.9	1.7	2.3	3.0	2.8	2.5
	C	3.0e-1	2.1e-1	1.1e+1	1.1	3.7e-1	2.8e-1	3.6e-1
3	s	3.0	3.8	4.4	3.5	3.5	1.9	2.1
	C	1.2e-1	3.6e-1	6.4e-2	2.7e-1	1.8	1.6e+1	7.7

LS-CF on the Ball

q		$\omega \equiv 1$			$\omega(\mathbf{x}) = \ \mathbf{x}\ _2^{1/2}$		
		equid.	uniform	Halton	equid.	uniform	Halton
2	s	2.5	1.6	3.1	2.5	2.3	2.9
	C	1.7	1.8e+1	3.2e-1	1.7	4.0	6.4e-1
3	s	1.2	2.5	2.3	1.0	2.4	2.4
	C	5.9e+1	1.1e+1	8.9	9.0e+1	1.3e+1	1.0e+1

 ℓ^1 -CF on the Ball

q		$\omega \equiv 1$			$\omega(\mathbf{x}) = \ \mathbf{x}\ _2^{1/2}$		
		equid.	uniform	Halton	equid.	uniform	Halton
2	s	2.5	2.2	2.6	2.5	3.1	2.6
	C	9.9e-1	1.5	5.0e-1	1.0	1.8e-1	4.7e-1
3	s	1.8	2.8	3.0	1.6	2.8	2.8
	C	1.3e+1	1.9	8.2e-1	2.6e+1	1.6	1.2

Table 1: LS fit for the parameters C and s in the model $N = Cd^s$

exponential parameter s is smaller, the multiplicative parameter C increases, and vice versa. This indicates that the proposed methods are fairly robust against different weight functions and domains. Figure 2 further illustrates this by displaying the DoE d of the LS- and ℓ^1 -CF for increasing N . Note that in all cases the ℓ^1 -CF achieves at least the same DoE—if not even a higher—compared to the LS-CF. This is in accordance with the ℓ^1 weights to minimize the stability measure κ while the LS weights minimize a weighted 2-norm.

6.2. Accuracy for Exact Data

Next, accuracy of the proposed LS- and ℓ^1 -CF for two different test cases without any noise is investigated.

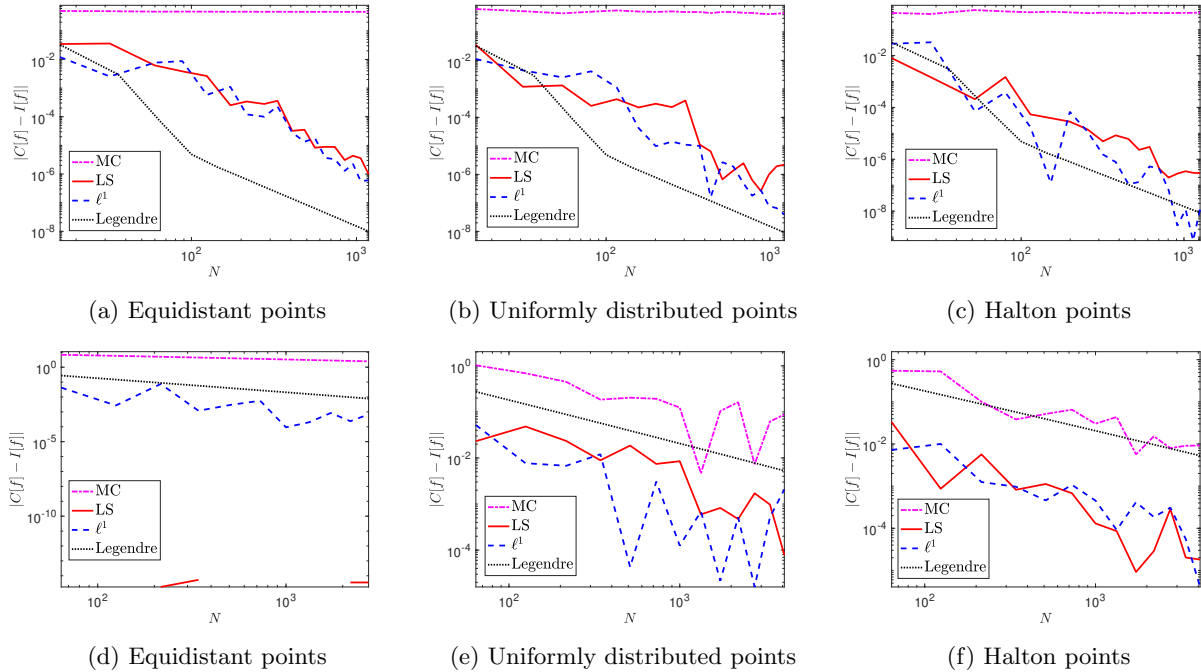


Figure 3: Upper figures: Errors for B_2 with ω and f as in (52). Lower figures: Errors for C_3 with ω and f as in (53).

The first test case is the two-dimensional ball B_2 with weight function ω and test function f given by

$$\omega(x, y) = \sqrt{\|(x, y)\|_2}, \quad f(x, y) = \frac{1}{1 + \|(x, y)\|_2^2}. \quad (52)$$

The results of the LS- and ℓ^1 -CF for equidistant, uniformly distributed and Halton points can be found in figures 3a, 3b, and 3c. The results are compared to the ones of the (quasi) MC method applied to the same set of data points as the LS- and ℓ^1 -CF as well as of the transformed product Legendre rule. The second test case is the three-dimensional cube C_3 together with

$$\omega(x, y, z) = \sqrt{1 - x^2} \sqrt{1 - y^2} \sqrt{1 - z^2}, \quad f(x, y, z) = \arccos(x) \arccos(y) \arccos(z). \quad (53)$$

The results of the LS- and ℓ^1 -CF for equidistant, uniformly distributed and Halton points can be found in figures 3d, 3e, and 3f. Again, the results are compared to the ones of the (quasi) MC method applied to the same set of data points as the LS- and ℓ^1 -CF as well as of the product Legendre rule. Note that for equidistant points (Figure 3d) the LS-CF is even below machine precision in many cases and therefore not displayed in the figure. Yet, this can be considered as an outlier; in most other cases, the LS- and ℓ^1 -CF perform similarly.

6.3. Accuracy for Noisy Data

Let us now perform the same tests as in the previous subsection, but introduce noise to the data. In both cases, i. i. d. uniform noise supported on $[-10^{-6}, 10^{-6}]$ is added. That is, noisy data \mathbf{f}^ε given by

$$f_n^\varepsilon = f(\mathbf{x}_n) + Z_n, \quad Z_n \in \mathcal{U}(-10^{-6}, 10^{-6}), \quad n = 1, \dots, N, \quad (54)$$

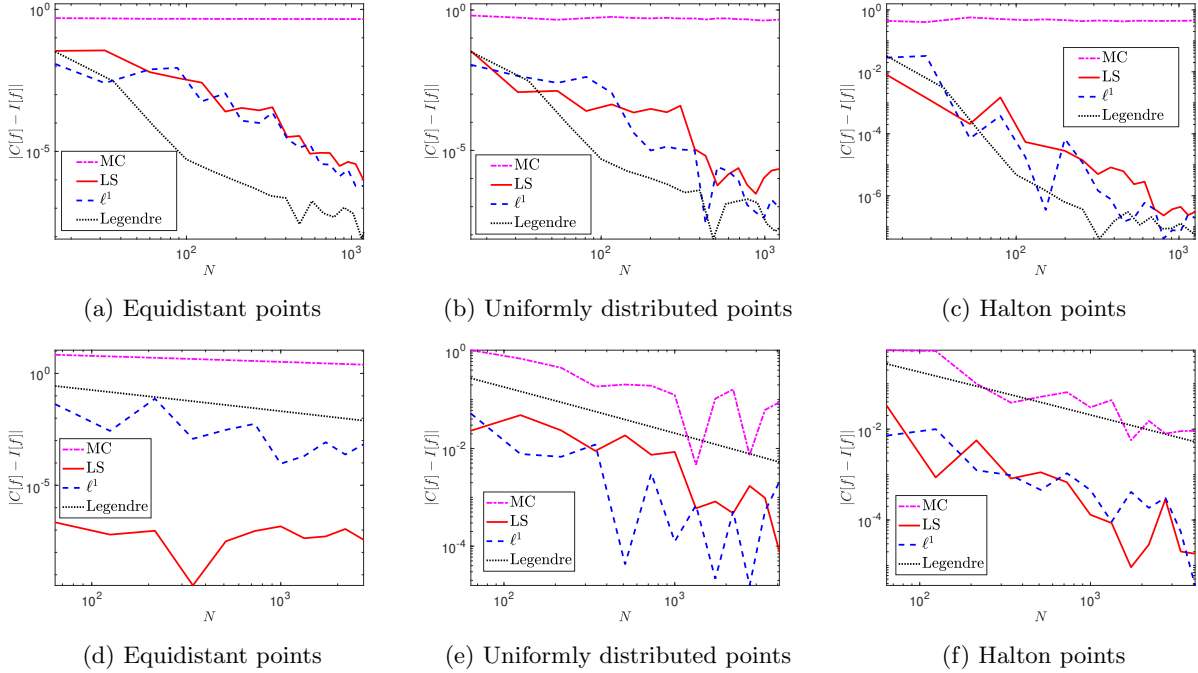


Figure 4: Errors when i. i. d. uniform noise $Z_n \in \mathcal{U}(-10^{-6}, 10^{-6})$ is added. Upper figures: B_2 with ω and f as in (52). Lower figures: C_3 with ω and f as in (53).

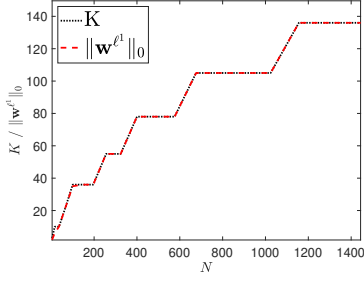
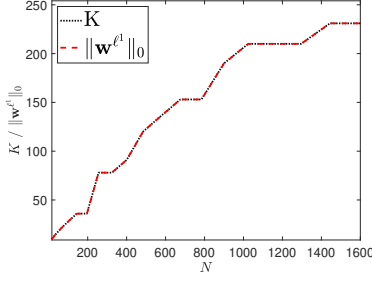
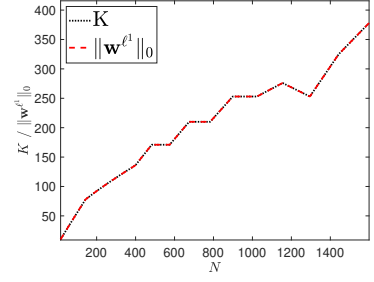
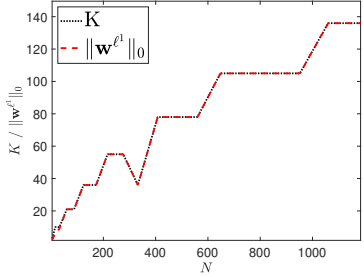
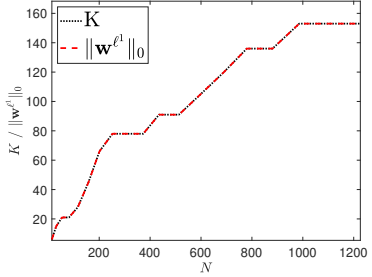
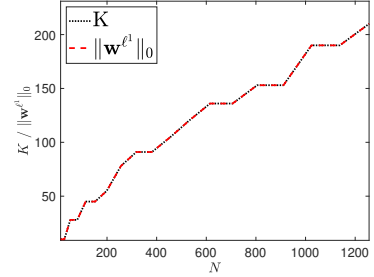
is considered, satisfying $\|\mathbf{f} - \mathbf{f}^\varepsilon\|_\infty \leq 10^{-6}$. Moreover, this noise is assumed to not be correlated to the data point \mathbf{x}_n or measurement $f(\mathbf{x}_n)$. In this case, none of the methods can be expected to yield an accuracy significantly lower than this uniform error bound.

This is also reflected by the corresponding numerical results reported in Figure 4. Note that all considered CF behave fairly robust against the introduction of noise. Of course, this is in accordance with all considered CFs having nonnegative cubature weights and therefore not allowing input errors to be drastically amplified by the CF. In figures 4a, 4b, and 4c, the error of the (quasi) MC might seem to not decrease at all. Yet, the rate of decrease is just considerably slower than for the other rules.

6.4. Number of Nonzero Weights of the ℓ^1 -CF

Finally, I would like to share a particularly noteworthy observation for the proposed ℓ^1 -CFs. As we noted before, the ℓ^1 -solution from the affine linear subspace of solutions W is a sparse solution in most cases [18]. This means that most of the cubature weights of the ℓ^1 -CF are expected to be zero and only a few are positive (by construction, there are no negative weights). Let us denote the number of nonzero weights of the ℓ^1 -CF by $\|\mathbf{w}^{\ell^1}\|_0$. This is a favorable property, since it enhances efficiency of the ℓ^1 -CF—at least once cubature weights are computed and the CF is applied to different data sets acquired at the same data points. Yet, when comparing $\|\mathbf{w}^{\ell^1}\|_0$ with the number of basis functions for which the ℓ^1 -CF is exact, $K = \binom{q+d}{q}$, we note that these are the same in many cases.

This finding is illustrated in Figure 5 for two different test cases. It means that the ℓ^1 -CF is able to provide us with a nonnegative interpolatory CF in many cases. To the best of my knowledge, the construction of nonnegative interpolatory CF for general classes of domains and weight functions has been of very limited success so far and essentially remains an open problem [12, 32]. Building up on the findings of the present work, in a forthcoming manuscript, I will describe the systematical construction of nonnegative interpolatory CF for quite general classes of domains and weight functions.

(a) C_2 with ω_1 and equidistant points(b) C_2 with ω_1 and uniform points(c) C_2 with ω_1 and Halton points(d) B_2 with ω_2 and equidistant points(e) B_2 with ω_2 and uniform points(f) B_2 with ω_2 and Halton pointsFigure 5: K and $\|\mathbf{w}^{\ell^1}\|_0$ versus N for C_2 with $\omega_1(x, y) = \sqrt{1-x^2}\sqrt{1-y^2}$ and B_2 with $\omega_2(x, y) = \sqrt{1-x^2+y^2}$

7. Summary

In this work, we developed two novel classes of CFs for experimental data (not fitting a known CF). Both of these are—by construction—ensured to be perfectly stable (in the sense of nonnegative only cubature weights) while also being able to achieve high DoE. The essential idea was to allow the number of data points N to be larger than the number of basis functions K for which the desired CF is exact. This yielded the SLE corresponding to the exactness conditions to become underdetermined and therefore to induce an $(N - K)$ -dimensional affine linear space of solutions W . Then, from this space W , cubature weights were selected that minimize certain norms corresponding to stability of the CF. Here, we investigated two options: (1) Minimization w. r. t. a weighted 2-norm, resulting in so-called LS-CFs. (2) Minimization w. r. t. the 1-norm, yielding so-called ℓ^1 -CFs. These CFs were developed for a predefined set of data points. Only half of the degrees of freedom could therefore be used for optimization of these CFs compared to many other CFs. Yet, we still observed the LS- and ℓ^1 -CFs to yield impressively accurate numerical results in a variety of different test cases (dimensions, domains, weight functions, point sets, and test functions). Finally, a forthcoming work will investigate how the proposed CFs can be utilized to construct nonnegative interpolatory CFs.

Appendix A. Moments of the Monomials

For the cube, the moments of the one-dimensional monomials, $I[x^k]$, are easy to compute for all cases:

$$C_1, \omega \equiv 1: \quad I[x^k] = \tilde{m}_k := \begin{cases} 0 & \text{if } k \text{ is odd,} \\ \frac{2}{k+1} & \text{otherwise,} \end{cases} \quad (A.1)$$

$$C_1, \omega(x) = \sqrt{1-x^2}: \quad I[x^k] = \hat{m}_k := \begin{cases} 0 & \text{if } k \text{ is odd,} \\ \frac{\pi}{2} & \text{if } k = 0, \\ \frac{(k-1)}{(k+2)} \hat{m}_{k-2} & \text{otherwise.} \end{cases}$$

The moments of the higher-dimensional monomials, $I[\mathbf{x}^{\mathbf{k}}]$ with multi-index $\mathbf{k} = (k_1, \dots, k_q)$, are respectively given by

$$I[\mathbf{x}^{\mathbf{k}}] = \tilde{m}_{k_1} \dots \tilde{m}_{k_q}, \quad I[\mathbf{x}^{\mathbf{k}}] = \hat{m}_{k_1} \dots \hat{m}_{k_q}. \quad (\text{A.2})$$

For the the ball, on the other hand, these are given by

$$B_q, \omega \equiv 1: \quad I[\mathbf{x}^{\mathbf{k}}] = \frac{2}{k_1 + \dots + k_q + q} \begin{cases} 0 & \text{if some } k_i \text{ is odd,} \\ \frac{\Gamma(\beta_1) \dots \Gamma(\beta_q)}{\Gamma(\beta_1 + \dots + \beta_q)} & \text{otherwise,} \end{cases} \quad (\text{A.3})$$

$$B_q, \omega(\mathbf{x}) = \sqrt{\|\mathbf{x}\|_2}: \quad I[\mathbf{x}^{\mathbf{k}}] = \frac{2}{k_1 + \dots + k_q + q + \frac{1}{2}} \begin{cases} 0 & \text{if some } k_i \text{ is odd,} \\ \frac{\Gamma(\beta_1) \dots \Gamma(\beta_q)}{\Gamma(\beta_1 + \dots + \beta_q)} & \text{otherwise,} \end{cases}$$

where $\beta_i = \frac{1}{2}(k_i + 1)$; see [20].

Acknowledgements

This work has benefited from helpful advice from Alina Glaubit, Dorian Hillebrand, and Simon-Christian Klein.

References

- [1] A. Ben-Israel and T. N. Greville. *Generalized Inverses: Theory and Applications*, volume 15 of *CMS Books in Mathematics*. Springer Science & Business Media, 2003.
- [2] C. B. Boyer and U. C. Merzbach. *A History of Mathematics*. John Wiley & Sons, 2011.
- [3] H. Brass and K. Petras. *Quadrature Theory: The Theory of Numerical Integration on a Compact Interval*. Number 178 in *Mathematical Surveys and Monographs*. American Mathematical Society, 2011.
- [4] R. E. Caflisch. Monte Carlo and quasi-Monte Carlo methods. *Acta Numerica*, 1998:1–49, 1998.
- [5] E. J. Candès, J. Romberg, and T. Tao. Robust uncertainty principles: Exact signal reconstruction from highly incomplete frequency information. *IEEE Transactions on Information Theory*, 52(2):489–509, 2006.
- [6] E. J. Candès, J. K. Romberg, and T. Tao. Stable signal recovery from incomplete and inaccurate measurements. *Communications on Pure and Applied Mathematics: A Journal Issued by the Courant Institute of Mathematical Sciences*, 59(8):1207–1223, 2006.
- [7] C. W. Clenshaw and A. R. Curtis. A method for numerical integration on an automatic computer. *Numerische Mathematik*, 2(1):197–205, 1960.
- [8] R. Cline and R. J. Plemmons. ℓ_2 -solutions to underdetermined linear systems. *SIAM Review*, 18(1):92–106, 1976.
- [9] R. Cools. Constructing cubature formulae: the science behind the art. *Acta Numerica*, 6:1–54, 1997.
- [10] R. Cools. An encyclopaedia of cubature formulas. *Journal of Complexity*, 19(3):445–453, 2003.
- [11] R. Cools, I. Mysovskikh, and H. Schmid. Cubature formulae and orthogonal polynomials. *Journal of Computational and Applied Mathematics*, 127(1-2):121–152, 2001.
- [12] P. J. Davis. A construction of nonnegative approximate quadratures. *Mathematics of Computation*, 21(100):578–582, 1967.
- [13] P. J. Davis and P. Rabinowitz. *Methods of Numerical Integration*. Courier Corporation, 2007.
- [14] N. G. De Bruijn. *Asymptotic Methods in Analysis*, volume 4. Courier Corporation, 1981.
- [15] J. Dick, F. Y. Kuo, and I. H. Sloan. High-dimensional integration: the quasi-Monte Carlo way. *Acta Numerica*, 22:133, 2013.
- [16] D. L. Donoho. Compressed sensing. *IEEE Transactions on Information Theory*, 52(4):1289–1306, 2006.
- [17] D. L. Donoho. For most large underdetermined systems of equations, the minimal ℓ_1 -norm near-solution approximates the sparsest near-solution. *Communications on Pure and Applied Mathematics: A Journal Issued by the Courant Institute of Mathematical Sciences*, 59(7):907–934, 2006.
- [18] D. L. Donoho. For most large underdetermined systems of linear equations the minimal ℓ_1 -norm solution is also the sparsest solution. *Communications on Pure and Applied Mathematics: A Journal Issued by the Courant Institute of Mathematical Sciences*, 59(6):797–829, 2006.
- [19] D. L. Donoho and M. Elad. Optimally sparse representation in general (nonorthogonal) dictionaries via ℓ^1 minimization. *Proceedings of the National Academy of Sciences*, 100(5):2197–2202, 2003.
- [20] G. B. Folland. How to integrate a polynomial over a sphere. *The American Mathematical Monthly*, 108(5):446–448, 2001.
- [21] W. Gautschi. Construction of Gauss–Christoffel quadrature formulas. *Mathematics of Computation*, 22(102):251–270, 1968.
- [22] W. Gautschi. *Numerical Analysis*. Springer Science & Business Media, 1997.
- [23] W. Gautschi. *Orthogonal Polynomials: Computation and Approximation*. Oxford University Press, 2004.

- [24] J. Glaubitz. *Introduction to Applied Mathematics*. Lecture notes, Dartmouth College, Hanover, NH, USA, 2020.
- [25] J. Glaubitz. jglaubitz/stableCFs. <https://doi.org/10.5281/zenodo.4018138>, 2020.
- [26] J. Glaubitz. *Shock Capturing and High-Order Methods for Hyperbolic Conservation Laws*. Logos Verlag Berlin GmbH, 2020.
- [27] J. Glaubitz. Stable high order quadrature rules for scattered data and general weight functions. *SIAM Journal on Numerical Analysis*, 58(4):2144–2164, 2020.
- [28] J. Glaubitz and A. Gelb. High order edge sensors with ℓ^1 regularization for enhanced discontinuous Galerkin methods. *SIAM Journal on Scientific Computing*, 41(2):A1304–A1330, 2019.
- [29] J. Glaubitz and P. Öffner. Stable discretisations of high-order discontinuous Galerkin methods on equidistant and scattered points. *Applied Numerical Mathematics*, 151:98–118, 2020.
- [30] J. Glaubitz, D. Rademacher, and T. Sonar. *Lernbuch Analysis 1: Das Wichtigste ausführlich für Bachelor und Lehramt*. Springer-Verlag, 2019.
- [31] G. H. Golub and C. F. Van Loan. *Matrix Computations*, volume 3. JHU Press, 2012.
- [32] S. Haber. Numerical evaluation of multiple integrals. *SIAM Review*, 12(4):481–526, 1970.
- [33] J. H. Halton. On the efficiency of certain quasi-random sequences of points in evaluating multi-dimensional integrals. *Numerische Mathematik*, 2(1):84–90, 1960.
- [34] E. Hlawka. Funktionen von beschränkter Variation in der Theorie der Gleichverteilung. *Ann. Mat. Pura Appl.*, 54(1):325–333, 1961.
- [35] F. E. Hoge and R. Swift. Oil film thickness measurement using airborne laser-induced water raman backscatter. *Applied Optics*, 19(19):3269–3281, 1980.
- [36] D. Huybrechs. Stable high-order quadrature rules with equidistant points. *Journal of Computational and Applied Mathematics*, 231(2):933–947, 2009.
- [37] A. R. Krommer and C. W. Ueberhuber. *Computational Integration*. SIAM, 1998.
- [38] V. I. Krylov and A. H. Stroud. *Approximate Calculation of Integrals*. Courier Corporation, 2006.
- [39] L. Kuipers and H. Niederreiter. *Uniform Distribution of Sequences*. Courier Corporation, 2012.
- [40] J. Matt. *Constrained minimum ℓ^1 -norm solutions of linear equations*. MATLAB Central File Exchange, 2020. Version 1.1.0.3.
- [41] J. C. Maxwell. On approximate multiple integration between limits of summation. In *Proc. Cambridge Philos. Soc.*, volume 3, pages 39–47, 1877.
- [42] N. Metropolis and S. Ulam. The Monte Carlo method. *Journal of the American Statistical Association*, 44(247):335–341, 1949.
- [43] H. Niederreiter. *Random Number Generation and Quasi-Monte Carlo Methods*. SIAM, 1992.
- [44] F. W. J. Olver, A. B. Olde Daalhuis, D. W. Lozier, B. I. Schneider, R. F. Boisvert, C. W. Clark, B. R. Miller, B. V. Saunders, H. S. Cohl, and M. A. McClain. NIST Digital Library of Mathematical Functions. Release 1.0.26, March 15, 2020, 2020.
- [45] J. A. Reeger. Approximate integrals over the volume of the ball. *Journal of Scientific Computing*, 83:45, 2020.
- [46] S. Roman, S. Axler, and F. Gehring. *Advanced Linear Algebra*, volume 3. Springer, 2005.
- [47] A. Sard. Best approximate integration formulas; best approximation formulas. *American Journal of Mathematics*, 71(1):80–91, 1949.
- [48] A. H. Stroud. *Approximate Calculation of Multiple Integrals*. Prentice-Hall, 1971.
- [49] L. N. Trefethen. Is Gauss quadrature better than Clenshaw–Curtis? *SIAM Review*, 50(1):67–87, 2008.
- [50] L. N. Trefethen. Cubature, approximation, and isotropy in the hypercube. *SIAM Review*, 59(3):469–491, 2017.
- [51] L. N. Trefethen and D. Bau III. *Numerical Linear Algebra*, volume 50. SIAM, 1997.
- [52] Y. Tsaig and D. L. Donoho. Breakdown of equivalence between the minimal ℓ^1 -norm solution and the sparsest solution. *Signal Processing*, 86(3):533–548, 2006.
- [53] J. van der Corput. Verteilungsfunktionen. In *Proc. Akad. Amsterdam*, volume 38, page 6, 1935.
- [54] H. Weyl. Über die Gleichverteilung von Zahlen mod. eins. *Mathematische Annalen*, 77(3):313–352, 1916.
- [55] M. W. Wilson. Discrete least squares and quadrature formulas. *Mathematics of Computation*, 24(110):271–282, 1970.
- [56] M. W. Wilson. Necessary and sufficient conditions for equidistant quadrature formula. *SIAM Journal on Numerical Analysis*, 7(1):134–141, 1970.